AUTOPHAGY
2023, VOL. 19, NO. 4, 1332–1347
https://doi.org/10.1080/15548627.2022.2126614

Taylor & Francis
Taylor & Francis Group

RESEARCH PAPER

NLRC5 restricts dengue virus infection by promoting the autophagic degradation of viral NS3 through E3 ligase CUL2 (cullin 2)

Jiawei Hao[a], Jinqian Li[a,b], Zhenzhen Zhang[a], Yang Yang[a], Qing Zhou[a], Tiantian Wu[a], Tongling Chen[a], Zhongdao Wu[c], Ping Zhang[d], Jun Cui[e], and Yi-Ping Li [a,f]

[a]Institute of Human Virology, Department of Pathogen Biology and Biosecurity, and Key Laboratory of Tropical Disease Control of Ministry of Education, Zhongshan School of Medicine, Sun Yat-sen University, Guangzhou, Guangdong, China; [b]Key Laboratory of Tropical Translational Medicine of Ministry of Education, NHC Key Laboratory of Control of Tropical Diseases, School of Tropical Medicine, Hainan Medical University, Haikou, Hainan, China; [c]Parasitology Unit, Department of Pathogen Biology and Biosecurity, and Key Laboratory of Tropical Disease Control of Ministry of Education, Zhongshan School of Medicine, Sun Yat-sen University, Guangzhou, Guangdong, China; [d]Department of Microbiology and Immunology, Zhongshan School of Medicine, Sun Yat-sen University, Guangzhou, Guangdong, China; [e]MOE Key Laboratory of Gene Function and Regulation, State Key Laboratory of Biocontrol, School of Life Sciences, Sun Yat-sen University, Guangzhou, Guangdong, China; [f]Department of Infectious Diseases, The Third Affiliated Hospital of Sun Yat-Sen University, Guangzhou, Guangdong, China

ABSTRACT

NLRC5 has been reported to be involved in antiviral immunity; however, the underlying mechanism remains poorly understood. Here, we investigated the functional role of NLRC5 in the infection of a flavivirus, dengue virus (DENV). We found that the expression of NLRC5 was strongly induced by virus infection and IFNB or IFNG stimulation in different cell lines. Overexpression of NLRC5 remarkably suppressed DENV infection, whereas knockout of *NLRC5* led to a significant increase in DENV infection. Mechanistic study revealed that NLRC5 interacted with the viral nonstructural protein 3 (NS3) protease domain and mediated degradation of NS3 through a ubiquitin-dependent selective macroautophagy/autophagy pathway. We demonstrated that NLRC5 recruited the E3 ubiquitin ligase CUL2 (cullin 2) to catalyze K48-linked poly-ubiquitination of the NS3 protease domain, which subsequently served as a recognition signal for cargo receptor TOLLIP-mediated selective autophagic degradation. Together, we have demonstrated that NLRC5 exerted an antiviral effect by mediating the degradation of a multifunctional protein of DENV, providing a novel antiviral signal axis of NLRC5-CUL2-NS3-TOLLIP. This study expands our understanding of the regulatory network of NLRC5 in the host defense against virus infection.

ARTICLE HISTORY
Received 28 March 2022
Revised 15 September 2022
Accepted 15 September 2022

KEYWORDS
Antiviral immunity; *flavivirus*; selective autophagy; TOLLIP; ubiquitination

Introduction

Dengue is the most prevalent arthropod-borne viral disease caused by dengue virus (DENV) infection, and it was one of the 10 threats to global health announced by World Health Organization in 2019 [1]. Four serotypes of DENV (DENV-1 to DENV-4) sustain the transmission cycle in humans and cause epidemics in more than 120 countries, with 400 million cases of DENV infection each year [2–5]. DENV infections result in a spectrum of diseases ranging from dengue fever with mild symptoms to severe dengue including dengue shock syndrome and dengue hemorrhagic fever [6]. To date, there are no specific antiviral drugs against DENV infection, and DENV and other flaviviruses continue to pose critical threats to the world [7].

DENV belongs to the *Flavivirus* genus of the *Flaviviridae* family, with a single-stranded positive-sense RNA genome of ~11 kilobases [8]. The RNA genome encodes one open reading frame (ORF) and the 5'- and 3'- untranslated regions (UTRs) [9]. The ORF is translated into a polyprotein, which is cleaved into three structural proteins (capsid, C; precursor membrane, prM; and envelope, E) and seven nonstructural proteins (NS1, NS2A, NS2B, NS3, NS4A, NS4B, and NS5) [10]. The structural proteins compose mature and extracellular virus particles, while nonstructural proteins are believed to express only within the infected cells in close association with cellular membranes and be mainly involved in viral genome replication, translation, and interaction with host factors. NS3 protein possesses RNA helicase and nucleotide triphosphatase activity, and together with its cofactor NS2B, is involved in processing of the viral polyprotein. Although it is known that replication of DENV occurs at the surface of endoplasmic reticulum (ER) membrane, forming the so-called replication complex, which consist of intracellular membrane, viral proteins and RNA, and cell factors [11–14], the interactions and regulations of host factors with viral proteins are not completely understood.

The nucleotide-binding oligomerization domain (NOD)-like receptors (NLRs) are a family of cytoplasmic pattern recognition receptors (PRRs), which play critical roles in innate immunity against microbial infection [15]. Typically, the NLRs contain an *N*-terminal caspase activation and recruitment domain (CARD) or pyrin domain, a central domain NACHT (a nucleoside triphosphatase domain; an

CONTACT Yi-Ping Li lyiping@mail.sysu.edu.cn Institute of Human Virology, Department of Pathogen Biology and Biosecurity, and Key Laboratory of Tropical Disease Control of Ministry of Education, Zhongshan School of Medicine, Sun Yat-sen University, Guangzhou, Guangdong 510080, China
Supplemental data for this article can be accessed online at https://doi.org/10.1080/15548627.2022.2126614

acronym standing for NAIP [neuronal apoptosis inhibitor protein], CIITA [MHC class II transcription activator], HET-E [incompatibility locus protein from *Podospora anserina*] and TEP1 [telomerase associated protein 1; also referred to as NOD domain]), and a C-terminal leucine-rich repeat (LRR) domain [16]. NLRC5 (NLR family CARD domain containing 5) is the largest member of the NLR family and abundantly expressed in immune cells [17], involved in inflammasome pathway, antigen presentation, and pathogen defense [18–20]. Our previous studies have demonstrated that NLRC5 is able to strongly inhibit NFKB/NF-κB-dependent responses and RIGI/RIG-I-like receptor-mediated type I interferon (IFN-I) responses by interacting with CHUK/IKKα-IKBKB/IKKβ and IFIH1/MDA5 [21–23]. Other studies showed that NLRC5 acts as a transcriptional regulator of MHC class I genes and is involved in RIGI- and IFN-, MHC-dependent antiviral responses [19,24–28]. Viruses have developed various strategies to counteract the function of NLRC5, such as SARS-CoV-2 [29]. Together, existing reports have exhibited a complex interplay between NLRC5 and virus infection, including positive and negative regulation of NLRC5 in the antiviral immune responses [27,30,31]. Moreover, the antiviral effect of NLRC5 reported is achieved through regulating host immune responses, while whether NLRC5 directly acts on viral antigens has not been studied.

Macroautophagy/autophagy, a major type of autophagy, is a highly conserved intracellular metabolism process, by which damaged organelles, misfolded, or aggregated proteins and invading pathogens are sent to lysosome for degradation or recycling [32–34]. Although autophagy was previously viewed as a nonselective bulk degradation process, several forms of selective autophagy have been well recognized to date [35]. In selective autophagy, the substrates are targeted by a variety of cargo receptors, including SQSTM1/p62, CALCOCO2/NDP52, OPTN, NBR1, BNIP3 L/NIX, TOLLIP, etc [36–39]. The receptors recognize the ubiquitinated substrate proteins and directly bind to MAP1LC3/LC3 (microtubule associated protein 1 light chain 3) to control protein degradation by selective autophagy [40]. In addition to physiological functions, selective autophagy has been found to suppress the *in vitro* infection of herpes simplex virus type 1 [41], hepatitis C virus [42], and porcine epidemic diarrhea virus [43] by degrading the viral proteins. Conversely, autophagy was also found to promote porcine reproductive and respiratory syndrome virus replication by preventing autophagosome and lysosome fusion [44]. Recent studies showed that autophagy restricted the infection of Zika virus (ZIKV) in *Drosophila* brain [45] but increased ZIKV replication in cultured cells [46]. Although autophagy has been known to play important roles in virus infection [47], it is still unknown whether autophagy is involved in the crosstalk between virus infection and NLRC5.

Here, we discovered that NLRC5 acted as an antiviral factor by targeting DENV NS3 through selective autophagy-mediated degradation. NLRC5 was upregulated during DENV infection and then recruited the E3 ligase CUL2 to catalyze the K48-linked ubiquitin chains on NS3. Our findings demonstrate a novel antiviral mechanism of NLRC5, by which it suppresses RNA virus infection through selective autophagy pathway.

Results

NLRC5 was upregulated by DENV infection and IFNB-IFNG stimulations

As the underlying mechanism of NLRC5 in antiviral responses remains unclear and controversial [19,30], here we aimed to elucidate the functional role of NLRC5 during virus infection. Initially, we investigated whether NLRC5 expression is disturbed by virus infection. We infected A549 cells with DENV-2 strain 16681 and found that virus infection markedly increased the expression of NLRC5 in a dose- and time-dependent manner (Figure 1A, B). The levels of DENV infection were also determined by measuring viral RNA levels in infected cells (Figure 1C). To investigate whether NLRC5 was upregulated by DENV-2 infection in other cell lines, we infected 293T, HUVEC, and THP-1 cells with DENV-2, and found that NLRC5 was also upregulated in these cells during DENV infection (Figure 1D). Concomitantly, IFNB was also elevated as expected (Figure 1E). In addition, NLRC5 expression was induced upon IFNB and IFNG treatment in A549 cells (Figure 1F, G), in line with previous reports that IFNG stimulation upregulated NLRC5 expression [28,48,49]. These data showed that the NLRC5 in these cell lines are functional. Together, these data demonstrate that NLRC5 expression was significantly induced during DENV infection and IFN stimulation, indicating that NLRC5 may play a role in regulating flavivirus infection.

DENV infection was restricted by NLRC5

To explore the effect of NLRC5 on DENV infection, A549 cells were transfected with NLRC5-expressing plasmids or empty vector control (EV) and then infected with DENV. The results showed that DENV infection was markedly reduced in NLRC5-transfected A549 cells compared with EV-transfected cells, as indicated by western blotting using anti-DENV NS3 antibody (Figure 2A). The reduction of DENV infection, determined by both the NS3 protein (Figure 2B) and the released infectious virus titers (Figure 2C), was also observed in NLRC5-transfected Vero cells during the course of 24, 48, and 72 h post transfection. To further confirm this observation, we generated an *NLRC5* knockout (KO) A549 cell line with one-nucleotide-insertion and four-nucleotide-deletion in the NLRC5 CARD domain, and this disruption did not apparently affect the cell viability and growth kinetics (Figure 2D). In DENV infection, NS3 protein level was significantly increased in the *NLRC5*-KO A549 cells compared to WT cells (Figure 2E). The corresponding culture supernatants were collected and subjected to plaque-forming unit assay (PFU), and the infectivity titers of DENV were increased in *NLRC5*-KO cells (Figure 2F).

To further confirm the increased DNEV infection was the effect of NLRC5 deficiency, we transfected the *NLRC5* KO A549 cells with plasmids expressing NLRC5 full-length (NLRC5-FL) as well as its three featured domains, CARD, NOD, and LRR, followed by DENV infection. The results showed that expression of NLRC5-FL or NLRC5-CARD significantly decreased the DENV infection (Figure 2G),

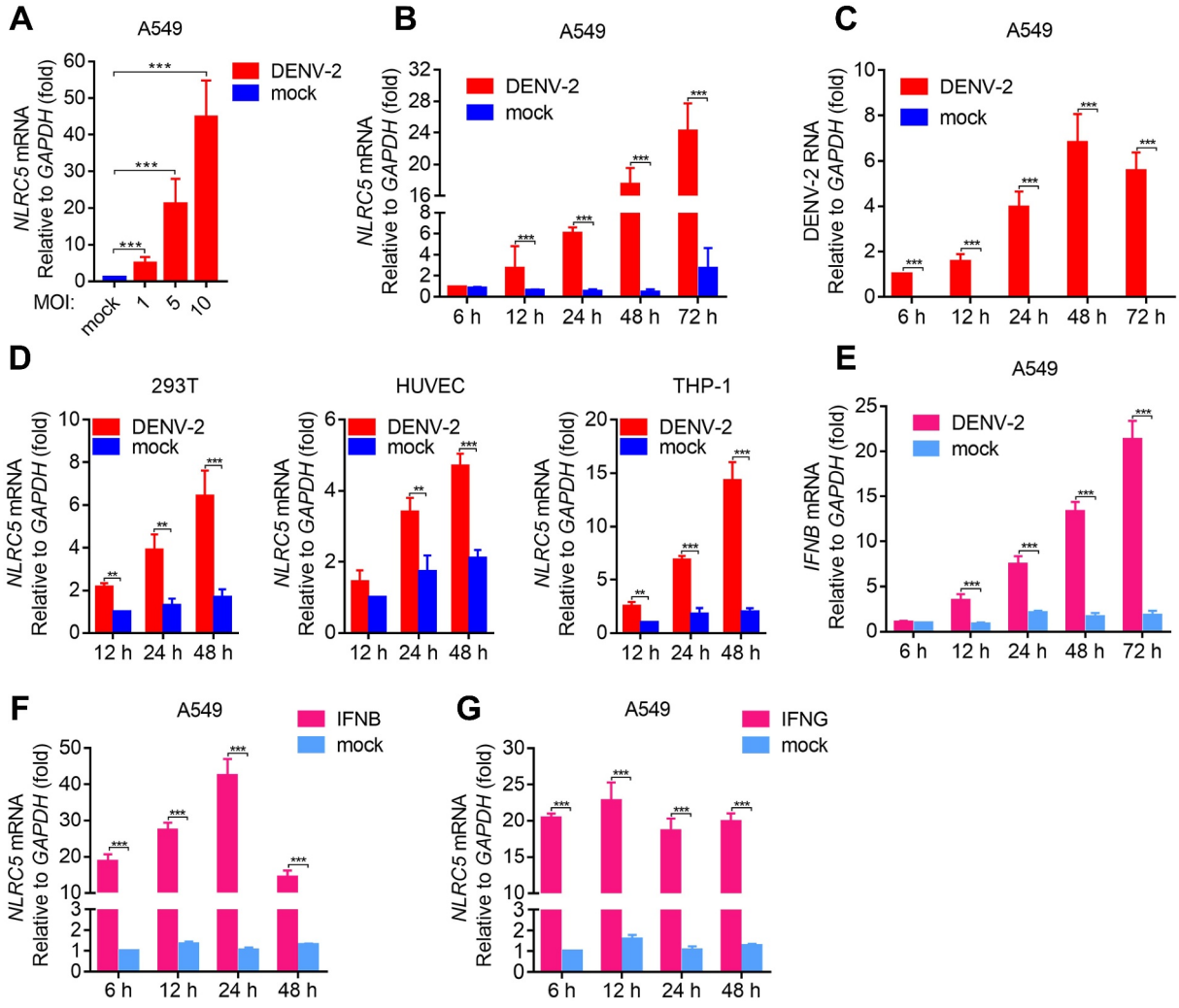

Figure 1. NLRC5 was upregulated by DENV infection and IFNB-IFNG stimulations. (**A**) A549 cells were infected with DENV-2 at an MOI of 1, 5, and 10 for 48 h. The cells were harvested and the *NLRC5* mRNA were quantitated by qRT-PCR. The fold changes of *NLRC5* were related to the internal control *GAPDH*. (**B**) A549 cells were infected with DENV-2 at an MOI of 2, and the cells were harvested at 6, 12, 24, 48, and 72 h post infection. The *NLRC5* mRNAs were quantitated by qRT-PCR, and its fold changes were related to *GAPDH*. (**C**) A549 cells were infected with DENV-2 at an MOI of 2 for 6, 12, 24, 48, and 72 h. The levels of DENV RNA were detected by qRT-PCR, relative to *GAPDH*. (**D**) HEK293T, HUVEC, and THP-1 cells were infected with DENV-2 (MOI = 2) for 12, 24, and 48 h. The *NLRC5* mRNAs were quantitated by qRT-PCR and presented as fold changes relative to *GAPDH*. (**E**) A549 cells was infected with DENV-2 at an MOI of 2 for 6, 12, 24, 48, and 72 h. The levels of *IFNB* mRNA were quantitated by qRT-PCR, relative to *GAPDH*. (**F**) A549 cells were stimulated with IFNB for 6, 12, 24, and 48 h at a concentration of 50 ng/ml, and then the *NLRC5* mRNAs were determined relative to *GAPDH*. (**G**) A549 cells were stimulated with IFNG for 6, 12, 24, and 48 h at a concentration of 100 ng/ml, and then *NLRC5* mRNAs were determined relative to *GAPDH*. In ***A-G*** panels, all the data are processed by Student's *t*-test and shown as means ± SEM of three independent experiments (*, $p < 0.05$; **, $p < 0.01$; and ***, $p < 0.001$). .

suggesting that NLRC5 specifically suppressed DENV infection. Together, these data strongly suggest that NLRC5 functioned as a restriction host factor for DENV infection, in which NLRC5 CARD domain plays a major role.

NLRC5 promoted autophagic degradation of DENV NS3

To determine the molecular mechanism by which NLRC5 suppressed DENV infection, we examined whether NLRC5 interacts with viral proteins. We performed co-immunoprecipitation (co-IP) assay by co-transfection of plasmids expressing NLRC5 and individual DENV protein and found that NLRC5 interacted with DENV E and NS3 proteins, but not with other viral proteins (Figure S1). Here, we proceed to further study NS3, as it is a highly conserved and multifunctional protein (e.g. ATPase/helicase and protease) important for DENV replication [50]. To examine whether NLRC5 affected NS3 protein, we co-transfected 293T cells with plasmids expressing NS3 and NLRC5 or control EGFP and found that NS3 protein level was markedly reduced in the presence of NLRC5, but not in the EGFP and mock transfections (Figure 3A), suggesting that the decrease of NS3 was NLRC5-specific; the interaction between NS3 and NLRC5 was also confirmed in the co-IP experiment (Figure 3B). We further demonstrated that NS3 reduction occurred at the protein level rather than transcription level, as the NS3 mRNA level was not affected by NLRC5 expression (Figure 3C). Moreover, NLRC5 specifically mediated the reduction of NS3, which became more apparent when NLRC5 level was gradually increased, while NS1 and NS5 levels were not affected by NLRC5 (Figure 3D). In contrast, siRNA-knockdown of *NLRC5* resulted in an increase of NS3

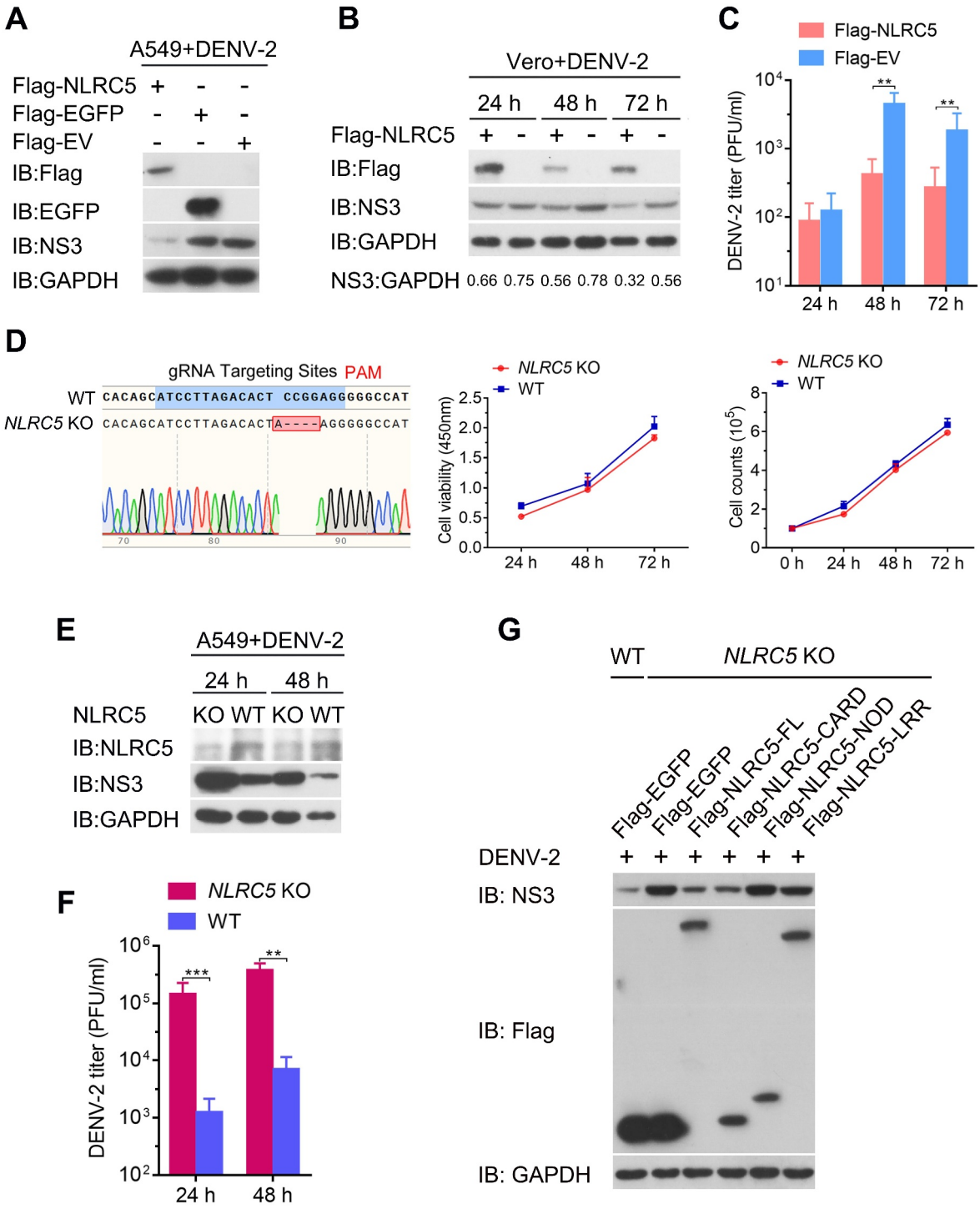

Figure 2. NLRC5 restricted DENV infection. (**A**) A549 cells were transfected with plasmids expressing Flag-NLRC5, Flag-EGFP, or Flag-vector (EV) for 12 h and then infected with DENV-2 at an MOI of 2 for 48 h. The expression levels of NLRC5, NS3, and control EGFP were detected by immunoblotting. (**B**) Vero cells were transfected with plasmid Flag-NLRC5 (refers to "+") or Flag-vector ("-") for 12 h and then infected with DENV-2 at an MOI of 2. The cells were harvested at 24, 48, and 72 h post infection. The expression levels of NLRC5, NS3, and GAPDH were detected by immunoblotting. (**C**) The infectivity titers of DENV-2 in culture supernatants from the experiment shown in panel ***B*** were determined by plaque-forming unit assay (PFU/ml). (**D**) Sequence analysis of wild-type (WT) and CRISPR-Cas9-mediated *NLRC5* knockout (KO) of A549 cell line (*NLRC5* KO), and the cell viability and growth kinetics of *NLRC5* KO cells in comparison with WT cells. (**E**) WT or *NLRC5* KO A549 cells were infected with DENV-2 for 24 and 48 h, and then the cells lysates were subjected to immunoblotting analysis. (**F**) The culture supernatants were collected from the experiment of panel ***E*** and determined for DENV-2 infectivity titers by PFU assay. (**G**) WT or *NLRC5* KO A549 cells were transfected with NLRC5 FL or truncated forms (see Figure ***4C*** for the schematic diagrams of truncated domains) for 12 h and then infected with DENV-2 at an MOI of 2 for 48 h. The cell lysates were analyzed by immunoblotting. In panels ***C, D,*** and ***F***, data are shown as mean ± SEM of three independent experiments (Student's *t*-test; **, $p < 0.01$; ***, $p < 0.001$).

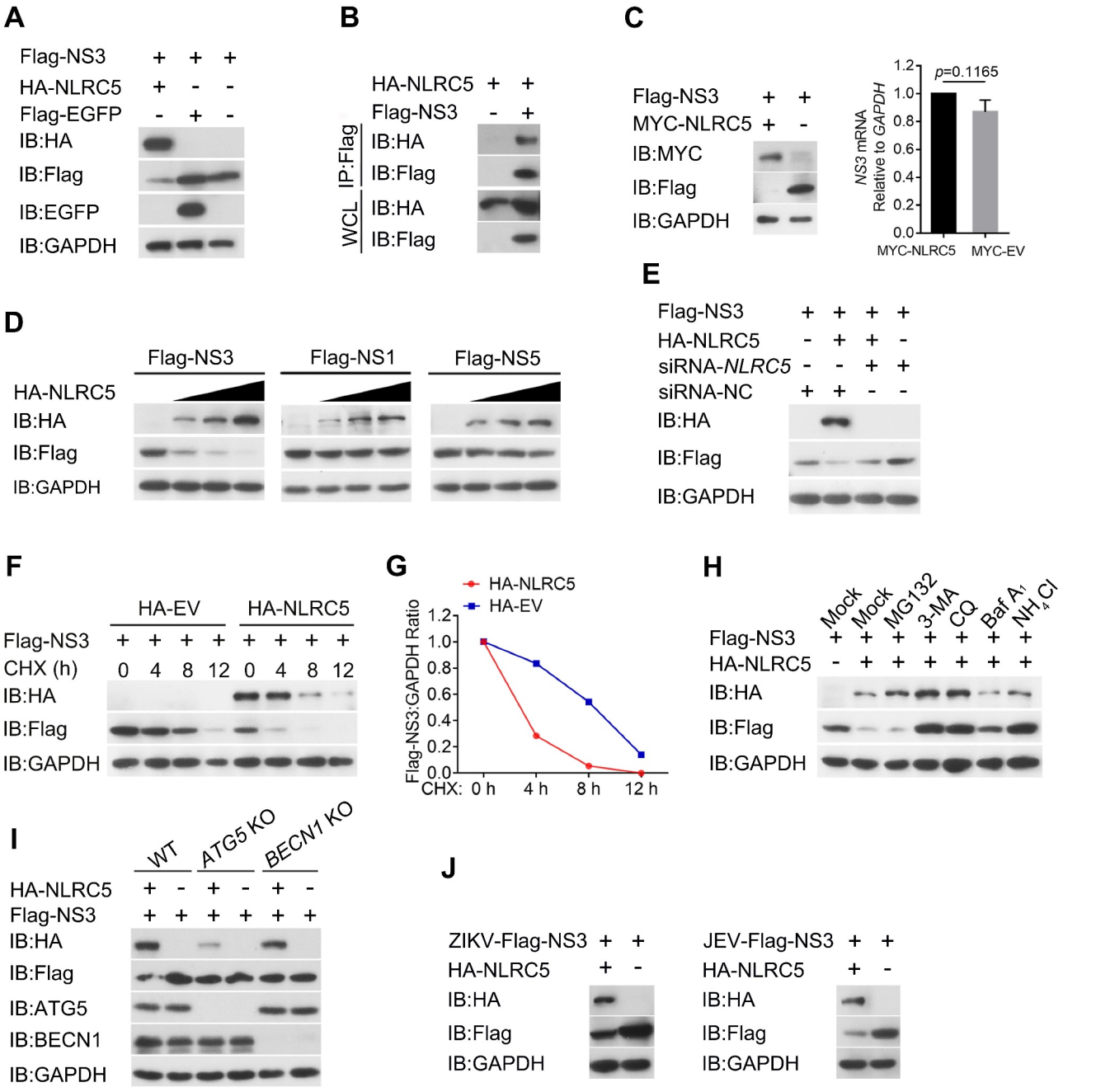

Figure 3. NLRC5 promoted autophagic degradation of DENV NS3 protein. (**A**) 293T cells were transfected with plasmids expressing Flag-NS3 and HA-NLRC5 or Flag-EGFP for 24 h, and the cell lysates were subjected to SDS-PAGE and immunoblotting analysis with antibodies indicated. (**B**) 293T cells were transfected with plasmids expressing Flag-NS3 and HA-NLRC5 for 24 h, and the cells were lysed and used for co-IP experiments. The whole cell lysates (WCL) and immunoprecipitates were analyzed by immunoblotting with Flag- and HA-antibodies. (**C**) 293T cells were co-transfected with plasmids expressing Flag-NS3 and MYC-NLRC5 for 24 h, and then the protein and mRNA levels of NS3 were detected by western blot and qRT-PCR, respectively. (**D**) 293T cells were co-transfected with each of Flag-NS3, Flag-NS1, or Flag-NS5 and an increasing amount of HA-NLRC5 (wedge, 0, 100, 300, and 600 ng) for 24 h. The cell lysates were analyzed by immunoblotting. (**E**) 293T cells were co-transfected with plasmids expressing Flag-NS3 and HA-NLRC5 for 12 h, followed by transfection of *NLRC5*-specific or control siRNAs for 24 h. The cell lysates were analyzed by immunoblotting. (**F**) 293T cells were co-transfected with Flag-NS3 and HA-NLRC5 or vector HA-EV for 24 h, then the cells were treated with cycloheximide (CHX; 100 μg/mL) and harvested at the time points as indicated. The protein levels of NS3, NLRC5, and GAPDH were detected by immunoblotting. (**G**) Quantification of the levels of NS3 proteins shown in panel ***F***. The levels of NS3 proteins in HA-EV and HA-NLRC5 were related to the level of internal control GAPDH, respectively, and then the relative level of NS3 protein at 0 h (starting point) was arbitrarily set as 1. (**H**) 293T cells were co-transfected with Flag-NS3 and HA-NLRC5 for 18 h, then the cells were treated with MG132 (10 mM), 3-methyladenine (3-MA; 10 μM), chloroquine (CQ; 50 μM), bafilomycin A_1 (Baf A_1; 0.4 μM), or NH_4Cl (20 mM) for 6 h. The cell lysates were analyzed by immunoblotting. (**I**) 293T cells with WT or KO of *ATG5* or *BECN1* were co-transfected with Flag-NS3, with or without HA-NLRC5 for 24 h. The lysates were analyzed by immunoblotting. (**J**) 293T cells were co-transfected with plasmids expressing HA-NLRC5 and Flag-NS3 of ZIKV or JEV for 24 h. The cell lysates were analyzed by immunoblotting.

level (Figure 3E). To investigate whether the presence of NLRC5 accelerates the degradation of NS3, we performed cycloheximide (CHX) chase assay in 293T cells transfected with NS3 with or without NLRC5. After 24 h post transfection of NS3 with NLRC5 or with vector plasmid, CHX was added to the culture medium to block the protein synthesis. The results clearly showed that the degradation of NS3 became obviously faster when NLRC5 was expressed, compared to the vector transfection control (Figures 3F, G), thus further confirming that NLRC5 accelerated the degradation of NS3 protein.

There are two major intracellular protein degradation systems: the ubiquitin-proteasome system (UPS) and autophagy-lysosome pathway [51,52]. Thus, we explored which degradation system was adopted predominantly by NLRC5 to mediate NS3 degradation. To this end, 293T cells were co-transfected with plasmids expressing NS3 and NLRC5, and then treated individually with protease inhibitor MG132 or with autophagy inhibitors 3-MA, chloroquine (CQ), bafilomycin A_1 (Baf A_1), or NH_4Cl. The results showed that treatment of 3-MA, CQ, $BafA_1$, and NH_4Cl, but not MG132, restored NS3 protein (Figure 3H). Also, NLRC5-mediated NS3 degradation was abrogated by knockout of *ATG5* or *BECN1* (Figure 3I). ATG5 and BECN1 are two genes essential for autophagy activation, and knockout of *ATG5* or *BECN1* could block the autophagy pathway. Moreover, NLRC5 did not affect LC3 conversion, indicating that NLRC5 did not alter the overall autophagy flux (Figure S2A). Overexpression of NLRC5, NS3, and mNG (mNeongreen)-LC3 in A549 cells revealed that the majority of NS3 was distributed in a punctate pattern and was colocalized with mNG-LC3-containing puncta (Figure S2B). In addition, NLRC5 also colocalized with NS3 at lysosomes (Figure S2C). Together, these results suggest that NLRC5 prompted degradation of DENV NS3 protein through autophagy pathway.

As NS3 is a conserved and multifunctional protein among flaviviruses, we wondered whether NLRC5 could also lead to degradation of NS3 from other flaviviruses. By co-transfection of NLRC5 and NS3 of ZIKV or JEV, two mosquito-borne flaviviruses closely related to DENV, we found that NLRC5 also mediated degradation of NS3 proteins of ZIKV and JEV (Figure 3J), suggesting that NLRC5-mediated NS3 degradation may represent a common antiviral strategy against the infection of flaviviruses.

NLRC5 interacted with DENV NS3 protease domain

Since NLRC5 specifically mediated autophagic degradation of NS3 (Figure 3**H**, **I**), we wanted to determine if NLRC5 interacted with native NS3 during DENV infection. We transfected 293T cells with NLRC5, followed by DENV infection, and found that NLRC5 had an interaction with NS3 (Figure 4A). Moreover, confocal microscopy analyzing up to 20 cells demonstrated that NLRC5 and NS3 colocalized in the cytoplasm of A549 cells (Figure 4B). Noteworthily, NS3 protein showed a diffused distribution in the cells transfected with NS3 only, whereas NS3 became more cytoplasmic puncta, which largely colocalized with NLRC5, in the cells co-expressing both proteins (Figure 4B).

To identify which domain of NLRC5 is involved in the interaction with DENV NS3, we generated truncated NLRC5 proteins with only CARD (amino acids, aa 1–215), NOD (aa 216–517), or LRR (aa 518–1866) (also in Figure 2G) for co-IP experiment and found that all of three truncated forms of NLRC5 showed interaction with NS3 (Figure 4C). Next, to determine which region of NS3 was involved in the interaction, we generated NS3 truncations containing primarily protease domain (PD, aa 1–180) and helicase domain (HD, aa 181–618) for co-IP experiment with NLRC5. The results showed that NLRC5 interacted with NS3 PD but not HD region (Figure 4D). Since CARD, NOD, and LRR domains of NLRC5 all interacted with NS3 (Figure 4C), we further investigated whether all these domains caused reduction of NS3 and found that CARD domain played a main role in NS3 degradation (Figure S3). This result further confirms the observation above that expression of NLRC5 CARD domain suppressed DENV infection in the *NLRC5* KO A549 cells (Figure 2G). Together, these results demonstrate that NLRC5 interacted with viral NS3 protease domain, which may contribute to the suppression of DENV infection.

NLRC5 promoted the autophagic degradation of NS3 using cargo receptor TOLLIP

Accumulating evidences revealed that the cargo receptors play an important role in delivering substrates for selective autophagic degradation [37,53]. Since NLRC5 is not a cargo receptor, we hypothesized that NLRC5 might bridge NS3 to a cargo receptor for autophagic degradation. Thus, we attempted to identify the cargo receptor responsible for the autophagic degradation of NS3. Co-IP results revealed that NLRC5 interacted with the cargo receptors SQSTM1/p62, CALCOCO2/NDP52, and TOLLIP (Figure 5A), but NS3 only interacted with SQSTM1 and TOLLIP (Figure 5B). As SQSTM1 and TOLLIP may target corporately one cargo [54], we attempted to identify whether both or only one receptor was required for degradation of NS3. siRNA knockdown of *TOLLIP* apparently restored NS3 level to a high extent but slightly lower than the control (Figure 5C), while knockdown of *SQSTM1* had marginal effect (Figure 5D), suggesting that TOLLIP was essential in mediating autophagic degradation of NS3, without excluding that other cargo receptors may also be involved. In line with this result, CHX-chase experiment showed that degradation of NS3 in *TOLLIP*-knockdown cells was notably slower than that in control cells (Figure 5E,F). Hence, we conclude that TOLLIP acted as a cargo receptor involving in the NLRC5-mediated autophagic degradation of DENV NS3.

Human TOLLIP consists of an *N*-terminal TOM1 (target of myb1 membrane trafficking protein)-binding domain (TBD, amino acids [aa] 1–54), a central conserved phospholipid-binding domain 2 (C2, aa 55–181), and a C-terminal coupling of ubiquitin to endoplasmic reticulum degradation domain (CUE, aa 219–274) [55]. To determine which domain of TOLLIP bound to NS3, we constructed TOLLIP receptor truncations with deletion of TBD, CUE, or both domains and performed co-IP with NS3. The results clearly showed that TOLLIP interacted with NS3 through CUE domain (Figure 5G).

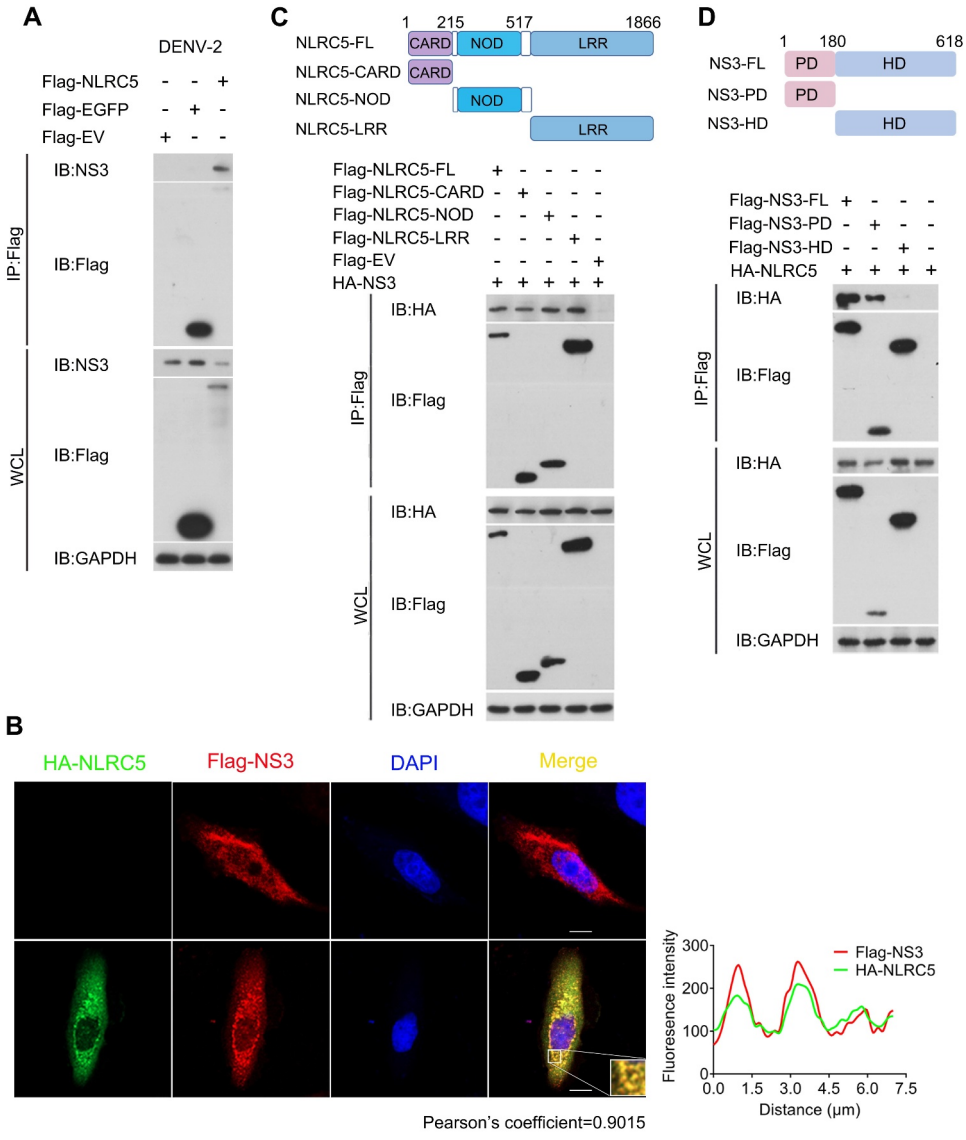

Figure 4. NLRC5 interacted with NS3 protease domain. (**A**) 293T cells transfected with plasmids Flag-NLRC5, Flag-vector (EV) or Flag-EGFP and infected with DENV-2 (MOI = 2) for 24 h. The cells were lysed, subjected to co-IP experiments, and analyzed by immunoblotting. (**B**) A549 cells were transfected with plasmids Flag-NS3 or HA-NLRC5 for 24 h, and then the cells were treated with Baf A_1 (0.4 μM) for 6 h. Treatment of Baf A_1 inhibited degradation of NS3 protein in the cells, thus facilitating detection of NS3 in IP experiment. The cells were fixed and immunostained with primary antibodies of anti-Flag- and anti-HA-tags, respectively, followed by the secondary antibody of Alexa Fluor 488 conjugated anti-mouse-IgG secondary antibody (green) and Alexa Fluor 555 conjugated anti-Rabbit-IgG secondary antibody (red); the nuclei were stained by DAPI (left panel). Scale bars: 10 μm. The fluorescence intensity profile of Flag-NS3 (red) and HA-NLRC5 (green) was plotted by GraphPad Prism 7 (right panel). The colocalization of NS3 and NLRC5 proteins was analyzed by Pearson's correlation coefficients with the Image J Plugin software. Data are representative of measurements using 20 cells from three independent experiments. (**C**) Schematic diagram of NLRC5 protein and its truncations CARD, NOD, and LRR (upper panel) and co-IP experiment (lower panel). 293T cells were co-transfected with HA-NS3 and individual plasmid of Flag-NLRC5 full-length (FL) or truncated versions and control vector for 24 h, and then the cells were treated with Baf A_1 (0.4 μM) for 6 h. The cells were lysed and used for co-IP. The WCL were immunoprecipitated with anti-Flag antibody and then immunoblotted with the antibodies indicated. (**D**) Schematic diagram of NS3 FL and its truncations containing protease domain (PD) and helicase domain (HD) (upper panel) and co-IP experiment (lower panel). 293T cells were co-transfected with HA-NLRC5 and individual plasmid of Flag-NS3 FL and its truncations for 24 h, and then the cells were treated with Baf A_1 (0.4 μM) for 6 h. The WCL and immunoprecipitates were analyzed by immunoblotting.

NLRC5 promoted the K48-linked ubiquitination of DENV NS3

Cargo receptors are committed to selective autophagy pathway by ubiquitin (Ub)-dependent mechanisms employing protein – protein interaction motifs [56,57]. CUE domain of TOLLIP is known to bind specifically to ubiquitin chains and recruit ubiquitinated substrates into the autolysosome [54]. Next, we examined the ubiquitination of NS3 and found that NLRC5 significantly increased the poly-ubiquitination of NS3 (Figure 6A). Seven types of poly-ubiquitination (K6, K11, K27, K29, K33, K48, K63) are involved in regulation of protein degradation, thus we attempted to analyze which type of ubiquitination occurred on NS3 protein in the presence of NLRC5. By co-transfection of NLRC5, NS3, and each of seven types of ubiquitin, we identified that NLRC5 significantly promoted the K48-linked ubiquitination of NS3 (Figure 6B).

To identify which NS3 region is responsible for ubiquitination and degradation, we co-transfected NS3 PD and HD truncations (from Figure 4D) together with NLRC5 and

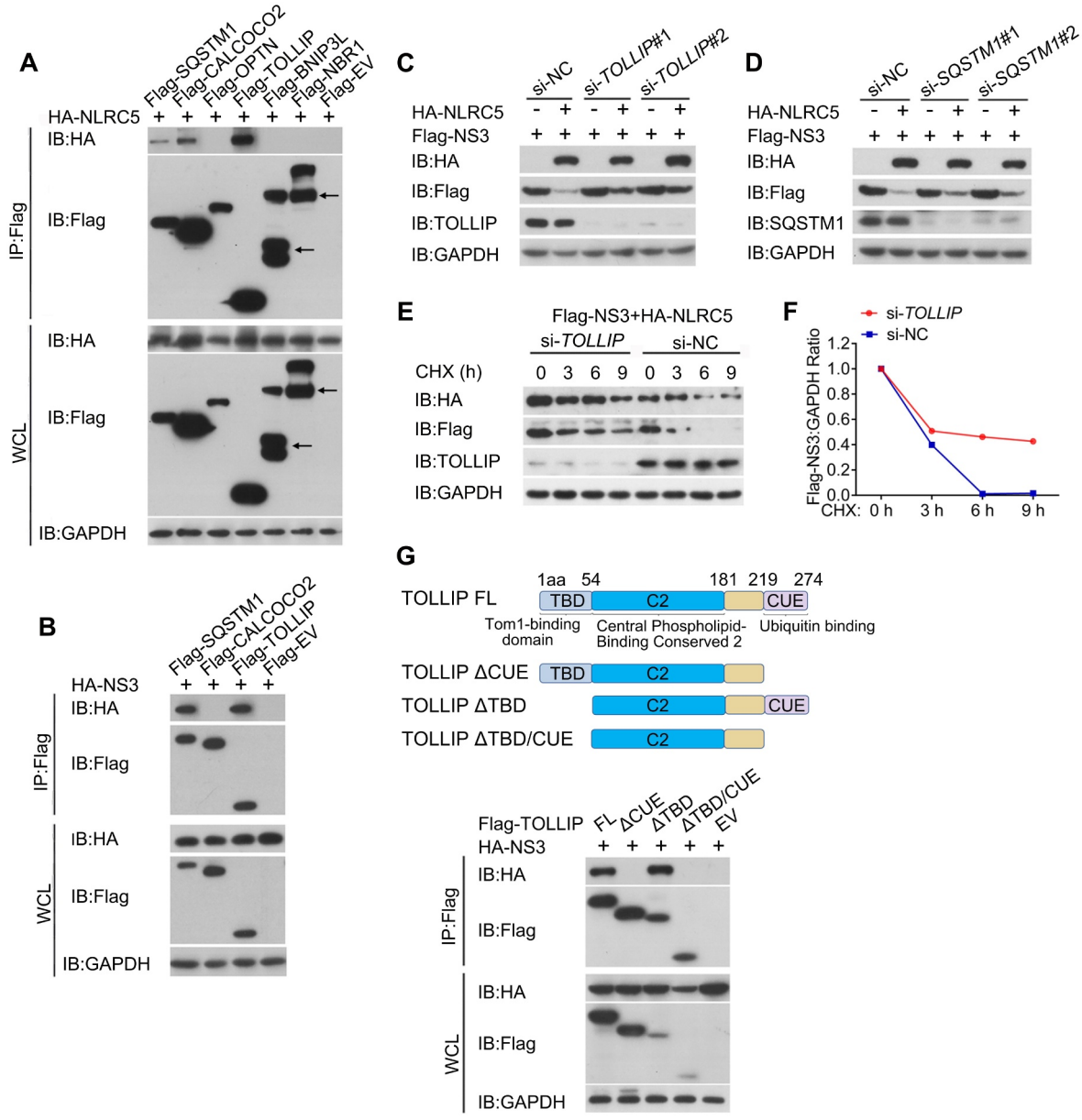

Figure 5. NLRC5 promoted the autophagic degradation of NS3 by cargo receptor TOLLIP. (**A**) 293T cells were co-transfected with HA-NLRC5 and Flag-tagged cargo receptors as indicated for 24 h, followed by immunoprecipitation with protein A/G beads. The WCL and IP precipitates were analyzed by immunoblotting with antibodies indicated. Arrows denote nonspecific bands appeared in transfections of Flag-BNIP3 L and Flag-NBR1. (**B**) 293T cells were co-transfected with HA-NS3 and Flag-tagged cargo receptors for 24 h. The WCL and IP precipitates were analyzed by immunoblotting. (**C**) 293T cells were transfected with Flag-NS3, with or without HA-NLRC5, and then the *TOLLIP*-specific siRNAs were transfected for 24 h. Scramble siRNAs (NC) were included as control. The cell lysates were analyzed by immunoblotting. (**D**) 293T cells were transfected with Flag-NS3, with HA-NLRC5 or vehicle vector ("-"), and then the *SQSTM1*-sepcific siRNAs (#1 & #2) were transfected for 24 h. Scramble siRNAs (NC) were included for control. The cell lysates were analyzed by immunoblotting. (**E**) 293T cells were co-transfected with Flag-NS3, HA-NLRC5, and scramble or *TOLLIP*-specific siRNAs for 24 h, and then the cells were treated with CHX (100 μg/mL) for 3, 6, and 9 h. The protein levels of NS3, NLRC5, TOLLIP, and GAPDH were detected by immunoblotting. (**F**) The protein levels of NS3 were quantitated and normalized to the level of GAPDH (from panel ***E***) at the time points indicated. The relative level of NS3 protein at 0 h (starting point) was arbitrarily set as 1. (**G**) Domain diagrams of TOLLIP receptor and co-IP analysis. 293T cells were transfected with HA-NS3 and each of TOLLIP full-length (FL) or truncated plasmids for 24 h, and the cell lysates were analyzed by co-IP and immunoblotting.

found that NS3-PD was degraded to a higher extent compared to NS3-HD in the presence of NLRC5 (Figure S4A and S4B), suggesting that degradation of NS3 was primarily attributed to PD domain. As NS3-PD domain contains 17 lysine residues, we attempted to identify the ubiquitination residue(s) of NS3-PD. We initially analyzed three subregions of NS3-PD, which contains 5, 6, and 6 lysine residues, respectively (Figure S4C). Co-transfection of three PD subregion constructs with clustered mutations of lysine (K)-to-arginine (R), as well as single K-to-R mutation, revealed that all three PD subregions could be degraded by NLRC5 (Figure S4D and data not shown). These data suggest that NLRC5-mediated autophagic degradation of NS3 was through K48-linked ubiquitination of multiple residues.

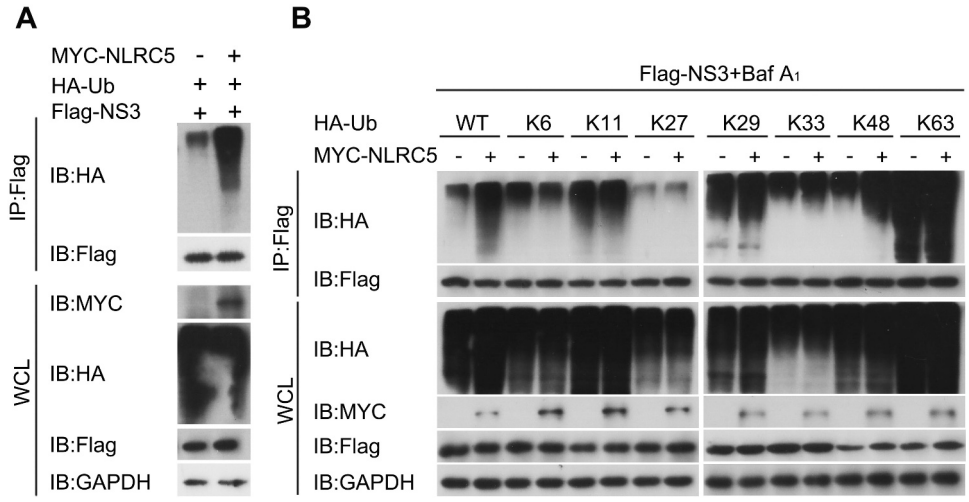

Figure 6. NLRC5 promoted the K48-linked ubiquitination of NS3. (**A**) 293T cells were co-transfected with plasmids expressing Flag-NS3, HA-ubiquitin (Ub), and MYC-vector ("-") or MYC-NLRC5, and then treated with Baf A_1 (0.4 μM) to maintain more NS3 protein for IP experiment. The cell lysates were used for immunoprecipitation and analyzed by immunoblotting. (**B**) 293T cells were co-transfected with plasmids expressing Flag-NS3 and each type of HA-Ub (K6, K11, K27, K29, K33, K48, and K63), with or without MYC-NLRC5 for 24 h. The cells were treated with Baf A_1 (0.4 μM) for 6 h, and then the cell lysates were immunoprecipitated and analyzed by immunoblotting.

NLRC5 recruited CUL2 to ubiquitinate DENV NS3

Since NLRC5 is not an E3 ubiquitin ligase, we reasoned that NLRC5 might function as an adaptor to recruit an E3 ligase to ubiquitinate NS3. To identify the E3 ubiquitin ligase(s) responsible for NS3 ubiquitination, we performed an affinity-isolation assay to search for the proteins that interacted with NS3 and NLRC5, and five extra bands in the NLRC5-affinity-isolation assay were analyzed by mass spectrometry (Figure S5A). A number of proteins were identified interacting with DENV NS3 when overexpressed NLRC5 in 293T cells,

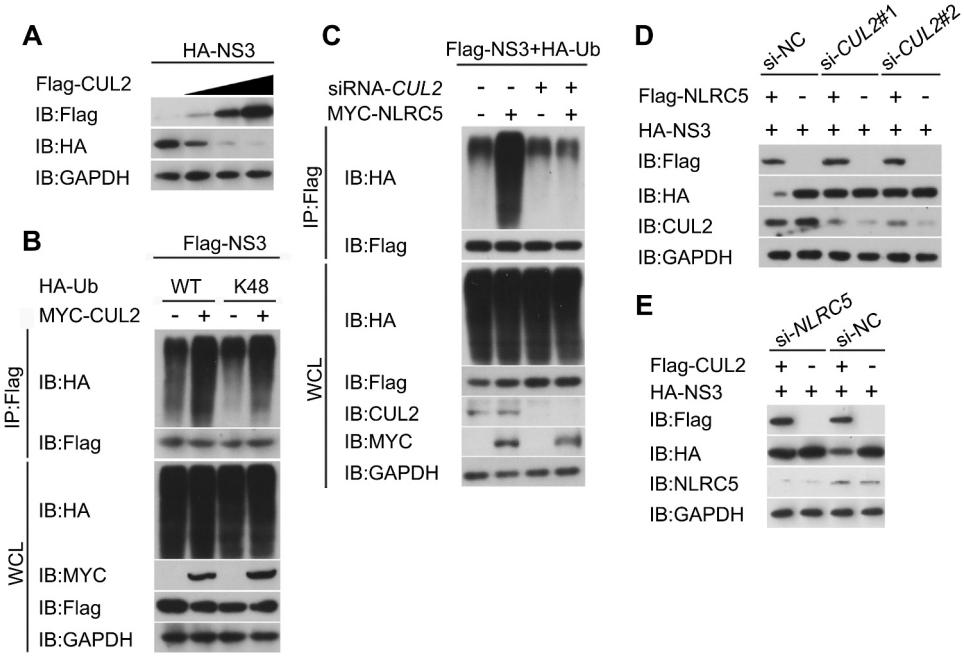

Figure 7. NLRC5 recruited the E3 ligase CUL2 to ubiquitinate DENV NS3 for autophagic degradation. (**A**) 293T cells were co-transfected with HA-NS3 and an increasing amount of Flag-CUL2 (wedge, 0, 100, 300, and 600 ng). The cell lysates were analyzed by immunoblotting. (**B**) 293T cells were co-transfected with Flag-NS3 and HA-tagged ubiquitin (WT and K48), together with MYC-CUL2 or the vehicle vector ("-"), and then treated with Baf A_1 (0.4 μM) for 6 h to inhibit NS3 degradation, thus enhancing NS3 detection in IP experiment. The cell lysates were immunoprecipitated with anti-Flag and immunoblotted with anti-HA antibody. (**C**) 293T cells were co-transfected with Flag-NS3 and HA-Ub, together with MYC-NLRC5 or the vehicle vector ("-"). Then, the CUL2-specific siRNAs were transfected and left for 24 h, followed by Baf A_1 (0.4 μM) treatment for 6 h. The cell lysates were immunoprecipitated with anti-Flag and immunoblotted with anti-HA antibody. (**D**) 293T cells were transfected with HA-NS3, together with Flag-NLRC5 or vehiclevector ("-"), and then the CUL2-specific siRNAs (#1 & #2) were transfected and left for 24 h. Scramble siRNAs (NC) were included as control. The cell lysates were analyzed by immunoblotting. (**E**) 293T cells were transfected with HA-NS3, together with Flag-CUL2 or vehicle vector ("-"), and then NLRC5-specific siRNAs were transfected and left for 24 h. Scramble siRNAs (NC) were included as control. The cell lysates were analyzed by immunoblotting.

including an E3 ligase CUL2 (cullin 2). We performed co-transfection of plasmids expressing CUL2, NS3, and NLRC5, and found that CUL2 did interact with NS3 and NLRC5 (Figure S5B and S5C).

To further verify whether CUL2 is the E3 ubiquitin ligase responsible for ubiquitination of NS3, we co-expressed 293T cells with NS3 together with different amount of CUL2. The results clearly showed that NS3 protein level was gradually decreased when increasing amount of CUL2 was given in the transfection (Figure 7A). Notably, ubiquitination analysis of NS3 demonstrated that CUL2 catalyzed the K48-linked poly-ubiquitination of NS3 (Figure 7B), and siRNA-knockdown of *CUL2* completely abrogated the NLRC5-dependent ubiquitination of NS3 protein (Figure 7C). In agreement with these results, siRNA-knockdown of *CUL2* also abrogated remarkedly the NLRC5-dependent degradation of NS3, as the level of NS3 was restored to that of the control cells without NLRC5 transfection (Figure 7D). Consistently, siRNA-knockdown of *NLRC5* also blocked NS3 degradation in the presence of CUL2 (Figure 7E). Together, these results strongly demonstrate that NLRC5 recruited E3 ligase CUL2 to ubiquitinate NS3 through K48-linked poly-ubiquitination for autophagic degradation.

NLRC5 restricted DENV infection through the NLRC5-CUL2-TOLLIP pathway

To further determine whether the NLRC5 restricts DENV infection through the NLRC5-CUL2-TOLLIP pathway, we performed DENV infection after siRNA-knockdown of *SQSTM1*, *TOLLIP*, or *CUL2* and found that overexpression of NLRC5 failed to suppress DENV infection after silencing either *TOLLIP* or *CUL2*, but NLRC5 inhibited DENV infection when *SQSTM1* was silenced or negative control siRNA were administrated (Figure 8A). Furthermore, knockout of *NLRC5* significantly reduced the extent of colocalization between NS3 protein and TOLLIP or NS3 and CUL2 (Figure 8B, C), whereas colocalization of NS3 and SQSTM1 was not changed (Figure 8D). In summary, these results further demonstrated that DENV NS3 protein was degraded through the NLRC5-CUL2-TOLLIP-autophagy pathway, thus the infection of DENV was suppressed.

Discussion

In this study, we discovered a novel antiviral mechanism of NLRC5 in response to virus infection. NLRC5 recruited E3 ligase CUL2 to catalyze the K48-linked poly-ubiquitination of DENV NS3 protease domain and mediated receptor TOLLIP-delivery of NS3 for autophagic degradation, thus the infection of DENV was severely suppressed. The NLRC5-CUL2-NS3-TOLLIP axis is a new pathway adding on the regulatory network of NLRC5 in antiviral response (Figure 9).

Previous studies have demonstrated that NLRC5 is a multifunctional protein contributing to type I IFN signaling and MHC class I gene expression, both of which are important in the antiviral response [19,27], but these antiviral effects resulted from immune responses rather than a direct-action of NLRC5. To date, it is still unknown whether NLRC5 directly acts on viral elements, RNA or proteins. Given the importance of flaviviruses, and its interaction with host factors was

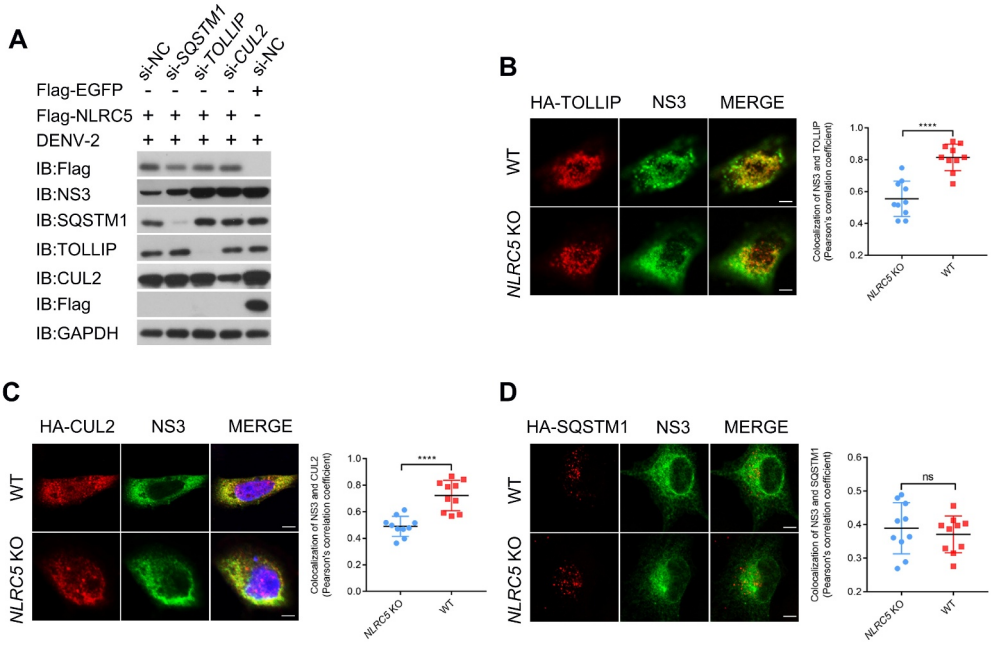

Figure 8. NLRC5 restricted DENV infection through the NLRC5-CUL2-TOLLIP-autophagy pathway. (**A**) 293T cells were transfected with plasmids expressing Flag-NLRC5 or Flag-EGFP and siRNAs targeting *SQSTM1*, *TOLLIP*, *CUL2*, as well as scramble control siRNAs (NC) for 12 h and then infected with DENV-2 at an MOI of 2 for 48 h. The cell lysates were analyzed by immunoblotting. (**B-D**) WT or *NLRC5*-KO A549 cells were transfected with HA-TOLLIP (**B**), HA-CUL2 (**C**), or HA-SQSTM1 (**D**) for 12 h and then infected with DENV (MOI = 2) for 48 h. The cells were fixed and immunoblotted with primary antibodies of HA-tag and NS3, respectively, followed by the secondary antibody of Alexa Fluor 488 conjugated anti-mouse-IgG secondary antibody and Alexa Fluor 555 conjugated anti-Rabbit-IgG secondary antibody. Scale bars: 10 μm. Pearson's correlation coefficients analyses were performed for DENV NS3 protein and HA-TOLLIP, HA-CUL2, or HA-SQSTM1. Data represent replicate measurements in at least 10 cells from one independent experiment.

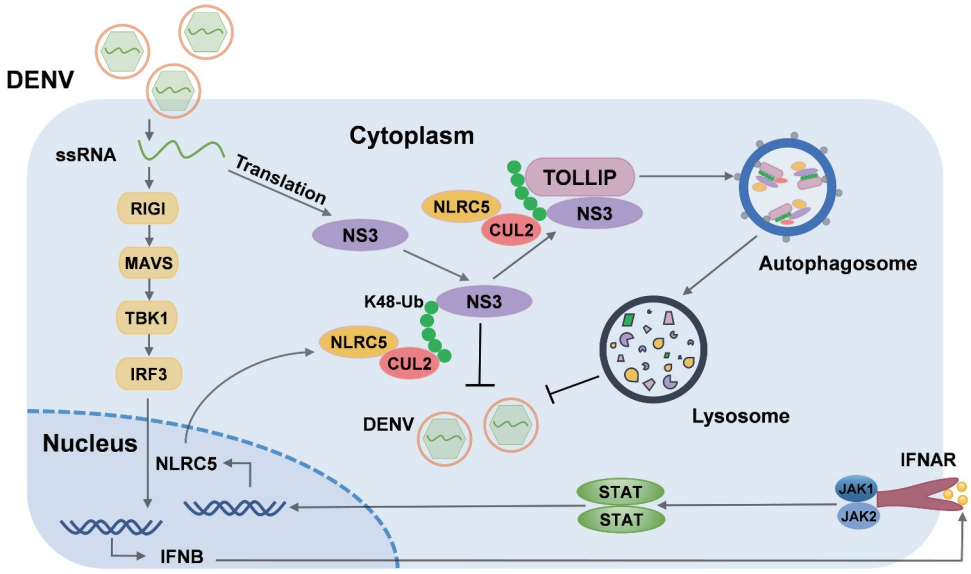

Figure 9. The working model of NLRC5-CUL2-NS3-TOLLIP axis inhibiting DENV infection. NLRC5 was upregulated by DENV infection, which in turn recruited the E3 ubiquitin ligase CUL2 to viral NS3 protein to mediate the K48-linked ubiquitination of NS3. The ubiquitinated NS3 protein was then recognized by the cargo receptor TOLLIP and delivered to the autolysosomes for degradation. Therefore, virus infection was suppressed in the cells.

largely unclear, we explored the underlying mechanism of NLRC5 by use of DENV as an infection model. As initial, we demonstrated that DENV infection and IFNB-IFNG stimulation significantly upregulated the expression of NLRC5 in different types of cell lines (Figure 1). Knockout or complement expression of NLRC5 apparently increased or inhibited DENV infection in different cells, respectively (Figure 2). Thus, we provided immediate evidence that NLRC5 acted as a restriction factor for DENV infection, and the infection models used in the study were robust and suitable for unveiling the antiviral regulation of NLRC5.

In addition to the removal and turnover of cellular components, autophagy also targets a variety of invading pathogens, such as bacteria and virus, and this type of autophagy is termed "xenophagy" [58]. To date, only few of NLR members were found to be involved in xenophagy as crucial defense proteins. NOD1 and NOD2 can induce autophagy to remove pathogens by recruiting ATG16L1 to the plasma membrane at the site of bacterial entry [59]. Mitochondrial proteins NLRX1 and TUFM form a complex to regulate virus-induced autophagy by interacting with ATG12–ATG5 and ATG16L1 [60]. Our study uncovered that NLRC5 is also involved in xenophagy process, and overexpression of NLRC5 did not affect autophagy flux (Figure S2A), suggesting that NLRC5 was not involved in autophagosome formation. These findings extended our knowledge on the functional role of NLR family members in host defense systems.

Accumulating evidences suggest that the interplay of selective autophagy and virus infection is extraordinarily complicated and largely unknown. In general, autophagy could be a defense mechanism against virus infection, however viruses might have developed strategies to usurp autophagy to benefit its infection; the proviral effect of autophagy has previously been documented for DENV [61]. Several studies attempted to investigate autophagy upon the infection of *Flaviviridae* viruses and found that NS2B3 of ZIKV and DENV were able to directly cleave the ER-localized autophagic receptor RETREG1/FAM134B (reticulophagy regulator 1), thus inhibiting RETREG1-mediated ER degradation and beneficial for viral replication [62]. DENV infection induces ER stress [63], increases the number of lipid droplets, and promotes accumulation of mature capsid protein on the surface of lipid droplets for viral replication [64]. In early infection, the autophagy flux is activated and supports DENV replication, but it was blocked at the later stage of infection to favor the production of infectious viral particles [65]. Studies also found that DENV and ZIKV were able to use autophagy components for post-RNA replication processes [66], and the Lyn-dependent mature DENV secretion via autophagosome-derived organelles was recently reported [67]. Collectively, these studies underscore the importance of autophagy in multiple stages of the flavivirus life cycle.

Conversely, viral proteins and host factors required for viral replication could be targeted to autophagic degradation, which is important for activation of antiviral response [68,69]. Different from these reports, we discovered that the viral NS3 protease became a major target of host defense through recognition of NLRC5, thus activating an autophagic degradation of NS3 and consequently inhibiting virus infection (Figure 3 and 4). NS3 is a multifunctional protein and conserved among the flaviviruses [70,71], containing mainly protease and helicase domains [71,72]. Helicase activity is essential to viral RNA replication [73], while primary function of protease domain, in complex with NS2B, is to execute the cleavage processing of viral polyprotein and other host proteins [74,75]. NS3 protease could counteract the CGAS-STING1 pathway for immune evasion [76]. In addition, NS3 was also found to be involved in virus assembly [77]. Therefore, degradation of NS3 should definitely be concomitant with the suppression of DENV infection, and targeting a multifunctional viral protein-like NS3 may be a consequence of evolution of host defense, as the

inhibitory effect could be achieved at multiple levels thus representing a cost-effective strategy. Host cells have evolved distinct mechanisms to degrade NS3 and NS2B3 of flaviviruses, such as TRIM69 mediates DENV NS3 degradation through ubiquitin-proteasome pathway [78,79], and TRIM5α induces the degradation of viral protease to restrict the replication of flaviviruses [73]. Viperin targets NS3 for proteasomal degradation to restrict ZIKV and tick-borne encephalitis virus replication [80], and C19orf66 induces lysosomal degradation of NS3 to interrupt ZIKV replication [81]. Discovery of autophagy pathway involved in the degradation of NS3 provides a novel insight into host defense against the infection of flaviviruses. Besides, targeting multifunctional NS3 protein may also explain the generalized effect of NLRC5 in host combating viral RNA replication, protein expression, and production of infectious virus progeny. It should be noted that three domains of NLRC5 showed interaction with NS3, but only CARD domain mediated NS3 degradation (Figure 4C and Figure S3). Previously, we found that several regions of NLRC5 could bind IKBKB/IKKβ, however only one region in LRR functioned to inhibit NFKB activity [21]. NLRC5 exists as a large member of NLR family, each of three domains binding to NS3 may not necessarily execute downstream degradation of NS3, however, this did not preclude other functional effects of the binding. In conclusion, our study displays a novel antiviral signaling by activating NLRC5-CUL2-NS3-antophagic pathway. Noting that, NLRC5 was also able to degrade the NS3 proteins from ZIKV and JEV (Figure 4H), thus suggesting potentially a broad-spectrum antiviral function of NLRC5 against multiple flaviviruses. However, this requires future investigations.

TOLLIP has been reported to function as a cargo receptor and to be involved in the clearance of protein aggregates [82], and it could cooperate with other cargo receptors (such as SQSTM1 and NBR1) to target one aggregate [54]. Here, we demonstrated that NS3 interacted with TOLLIP, through its ubiquitination domain CUE (Figure 5E), different from SQSTM1 and NBR1 receptors being UBA domain; this observation is in line with a previous report that ubiquitin recognized TOLLIP via CUE domain [54]. Noted that, TOLLIP receptor has not been found to be involved in the autophagic degradation of a viral protein, hence it is worth to explore its role in virus infection in the future. Besides, the fact that knockdown of TOLLIP restored NS3 level to a high extent but not comparable to the control (Figure 5C) may indicate the involvement of other cargo receptors in the degradation process of NS3 protein. Previous work reports that cargo receptor SQSTM1 could significantly suppress DENV replication and was depleted via proteasomal degradation in DENV-infected cells [65], whether the inhibitory effect of SQSTM1 on DENV replication involves autophagy pathway would be of interest in future study.

K48-linked ubiquitination is well recognized as a canonical signal for proteasome degradation, while K63-polyubiquitin is involved in autophagy degradation pathway [83,84]. However, a number of studies have demonstrated that both ubiquitination types are involved in autophagic degradation of substrates [85–87]. Moreover, cargo receptor TOLLIP CUE domain could interact with K48- and K63-linked polyubiquitin chains [54], further suggesting that K48-linked ubiquitination seem to prime proteins for multiple degradation pathways.

In summary, we demonstrated a novel mechanism of NLRC5 in antiviral defense by activating a NLRC5-CUL2-NS3-TOLLIP-autophagy axis to suppress virus infection, and this pathway may be commonly applied to combat flaviviruses.

Materials and methods

Antibodies and reagents

The antibodies were commercially available and used according to the manufacturers' instructions. Antibodies anti-NLRC5 (ab105411; 1:1000) and anti-TOLLIP (ab187198; 1:1000) were purchased from Abcam. Anti-DENV NS3 antibody (GTX124252; 1:2000) was purchased from GeneTex. Antibodies for horseradish peroxidase (HRP)-conjugated GAPDH/glyceraldehyde-3-phosphate dehydrogenase (HRP -60004; 1:6000), anti-Flag-tag (20543-1-AP; 1:5000), anti-MYC/c-Myc-tag (67447-1-Ig; 1:8000), anti-SQSTM1/p62 (18420-1-AP; 1:5000), anti-ATG5 (10181-2-AP; 1:1000), anti-BECN1 (11306-1-AP; 1:1000) were purchased from Proteintech Group. Anti-HA-tag antibody (M180–3; 1:6000) was purchased from MBL. Antibodies Goat anti-Mouse IgG (H+L) HRP Secondary Antibody (RM-3001; 1:5000) and Goat anti-Rabbit IgG (H+L) HRP Secondary Antibody (RM-3002; 1:5000) were purchased from Beijing Ray Antibody Biotech. Goat anti-Mouse IgG (H+L) Highly Cross-Adsorbed Secondary Antibody (Alexa Fluor® 488 dye) (A -12029; 1:1000) and Goat anti-Rabbit IgG (H+L) Highly Cross-Adsorbed Secondary Antibody (Alexa Fluor® Plus 555; A -32732; 1:1000) were purchased from Invitrogen.

Chemical reagents were purchased and used without further purification. 3-methyladenine (10 mM, 3-MA; M9281), chloroquine phosphate (50 μM, CQ; PHR1258), NH_4Cl (20 mM; 12125-02-9), and MG132 (10 μM; M8699) were from Sigma-Aldrich. Bafilomycin A_1 (0.4 μM, Baf A_1; S1413) and cycloheximide (100 μg/mL, CHX; S7418) was purchased from Selleck Chemicals. Protein A/G Sepharose beads (P001–3) were purchased from 7Sea Biotech. Recombinant Human IFNB (50 ng/ml; 300-02BC) and Recombinant Human IFNG (100 ng/ml; 300–02) were purchased from PeproTech. Lipofectamine 2000 (11668019) was purchased from Thermo Fisher Scientific.

Plasmids

The genes encoding viral proteins were amplified from the DENV-2 infectious clone 16681 (provided by Dr. Andrew Yueh, Institute of Biotechnology and Pharmaceutical Research, National Health Research Institutes, Taiwan, China) [88] by standard PCR procedure and cloned into the pCMV-3×Flag-1b vector (provided by Dr. Mengfeng Li, Sun Yat-sen Unviersity). Flag-tagged NLRC5, NBR1, OPTN, SQSTM1, CALCOCO2, TOLLIP, and BNIP3 L, and HA-tagged ubiquitin (Ub)-wild type (WT), K6, K11, K27, K29,

K33, K48, and K63 were previously reported [21,39]. HA- and MYC-tagged NLRC5 were constructed by cloning the *NLRC5* ORF into the pCMV-3×HA-1b and pCMV-3×MYC-1b vectors (modified from pCMV-3×Flag-1b vector), respectively. Plasmids with point mutations or truncations were constructed by overlapping PCR or chemically synthesis. All plasmid constructs were confirmed by sequence analysis.

Cell culture

HEK293T, A549, and Vero cells were maintained in our laboratory [89,90] and cultured in Dulbecco's modified eagle medium (DMEM; Gibco/Thermo Fisher Scientific, 2478988) with 10% fetal bovine serum (FBS; ExCell Bio, FSP500). HUVEC cells (provided by Dr. Yan Yuan, Sun Yat-sen University, China) and THP-1 cells (From Dr. Ping Zhang's laboratory, Sun Yat-sen University, China) were cultured in RPMI 1640 medium (Gibco/Thermo Fisher Scientific,11875093) with 20% and 10% FBS, respectively. All cells were maintained in the incubator with 5% CO_2 at 37℃.

Virus propagation, infection, and titration

To propagate DENV virus or to perform virus infection experiments, Vero, A549, or other cells were inoculated with DENV-2 strain 16681 with the multiplicity of infection (MOI) as indicated and cultured with 5% CO_2 at 37℃ for 2 h. Then, the inoculation medium was replaced with fresh medium, and the infected cultures were maintained in the incubator until the virus supernatant was collected for analysis. To determine the dose of DENV infection, we performed pilot studies and found that MOI of 2 gave better results without massive cell death during the course of experiments and thus was used for subsequent infection experiments.

DENV infectivity titers were determined by plaque forming assay using Vero cells. Briefly, Vero cells were inoculated with the 10-fold serial dilutions of DENV and inoculated into the cells for 2 h, the virus inoculum was then removed, and fresh DMEM containing 1% methylcellulose was added. After 4–5 days, cells were fixed with 4% paraformaldehyde and stained with 1% crystal violet. The plaques became visible and were manually counted, and the virus infectivity titers were presented as plaque forming units per milliliter (PFU/ml) of culture supernatant.

Quantitative reverse transcription PCR

Total RNAs were extracted from cells by use of Magzol (Magen, JJ153300). For the reverse transcription quantitative PCR (RT-qPCR), cDNA was generated with the HiScript II Q Select RT SuperMix for qPCR kit (Vazyme, R232–01) and was amplified by qPCR using ChamQ Universal SYBR qPCR Master Mix (Vazyme, Q711–02) with specific PCR primers (Table S1). The expression levels of genes of interest were normalized to that of respective internal control *GAPDH* and presented as fold change relative to the control. The analysis of each gene expression was repeated in at least three independent experiments.

Immunoprecipitation and immunoblot analysis

Immunoprecipitation (IP) was performed using HEK293T cells. The cells were lysed in low-salt lysis buffer (50 mM HEPES, pH 7.5, 150 mM NaCl, 1 mM EDTA, 1.5 mM $MgCl_2$, 10% glycerol, 1% Triton X-100 [TianJin DINGGUO Biotechnology, DH351-4]), supplemented with a protease inhibitor cocktail (Sigma-Aldrich, P8849-5 ML) and incubated with the appropriate antibodies plus protein A/G beads overnight. The beads were washed five times with the low-salt lysis buffer, and the immunoprecipitates were eluted from the beads with 1× sodium dodecyl sulfate (SDS) loading buffer (Invitrogen, 2417530) and resolved on 8 to 12% SDS-polyacrylamide gels (SDS-PAGE). Electrophoresis was done with 80 V for 30 min and then 120 V for 90 min. Proteins were transferred to polyvinylidene fluoride (PVDF) membranes (Bio-Rad, 1620177), followed by blocking with 5% skim milk and incubating with the appropriate antibodies, and then the protein bands were visualized by immobilon western chemiluminescent HRP substrate (Proteintech Group, PK10001).

Fluorescence microscopy

For fluorescence microscopy analysis, A549 cells were seeded in glass coverslips. The cells that have been transfected or virally infected were fixed with 4% paraformaldehyde for 30 min, permeabilized with 0.2% Triton X-100 for 20 min, and blocked with 1% bovine serum albumin (BSA; Huaqisheng Biotechnology, 38680326) in PBS (137 mM NaCl, 2.7 mM KCl, 10 mM Na_2HPO_4 12 H_2O, 2 mM KH_2PO_4, pH 7.4) for 30 min. The cells were incubated with the primary antibody overnight in 4℃, and then secondary antibodies and 4′,6-diamidino-2-phenylindole (DAPI; Invitrogen, 208 6723) for 1 h at room temperature in the dark. Intracellular fluorescence was captured by a confocal laser-scanning microscope (Carl Zeiss, LSM800) under a 63× oil-immersion objective. The images were processed for gamma adjustments using LSM Zen 2008 and ImageJ software (National Institutes of Health, USA). The fluorescence intensity profile of the indicated proteins was measured by using the GraphPad Prism 7 software (GraphPad Software). Pearson's correlation coefficient was calculated using the plugin for ImageJ [42].

Inhibitor treatment

HEK293T cells were transfected with plasmids for 24 h, and then the culture medium was replaced with fresh medium containing inhibitors. The cells were harvested after 6 h, and total cell lysates were subjected to SDS-PAGE and western blotting. MG132 (10 μM) was used to inhibit proteasome-mediated protein degradation. 3-MA (10 mM), CQ (50 μM), bafilomycin A_1 (Baf A_1, 0.4 μM), or NH_4Cl (20 mM) was used to inhibit autolysosome- or lysosome-mediated protein degradation.

Cycloheximide (CHX)-chase assays

HEK293T cells were transfected with plasmids for 24 h, then the medium was changed to fresh medium containing CHX (100 μg/mL; ACMEC, A14033729). The cells were harvested at 4, 8,

and 12 h, and total cell lysates were subjected to SDS-PAGE and subsequent western blotting to visualize the amount of NLRC5, NS3, and internal control GAPDH. The levels of NS3 proteins were normalized to respective GAPDH at each time point, by which the degradation rate of NS3 protein with or without the presence of NLRC5 were determined and then plotted using GraphPad Prism 7 (GraphPad Software).

RNA interference (RNAi) experiment

Small interference RNAs (siRNAs) targeting human *NLRC5*, *SQSTM1*, *TOLLIP*, and *CUL2* genes and scramble siRNA controls were designed and synthesized by GenePharma (Shanghai, China) (Table S2). siRNAs were transfected into the 293T and A549 cells for 6 h using Lipofectamine 2000 reagent (Invitrogen/Thermo Fisher Scientific, 11668019) according to the manufacturer's instructions.

Statistical analyses

Data are represented as mean ± SEM, and Student's *t*-test was used for all statistical analysis with the GraphPad Prism 7 software. Differences between two groups were considered significant when p value was less than 0.05.

Acknowledgement

We thank Dr. Andrew Yueh (National Health Research Institutes, Taiwan, China) for providing the DENV-2 infectious clone 16681, Dr. Yan Yuan (Sun Yat-sen University, Guangzhou, China) for HUVEC cells, Dr. Mengfeng Li (Sun Yat-sen University, Guangzhou, China) for pCMV-3×Flag-1b vector, Dr. Cheng-Feng Qin (Academy of Military Medical Sciences, Beijing, China) and Dr. Jincun Zhao (The First Affiliated Hospital of Guangzhou Medical University, Guangzhou, China) for full-length infectious cDNA of JEV.

Disclosure statement

No potential conflict of interest was reported by the author(s).

Funding

The work was supported by the National Key Research and Development Program of China [2020YFC1200100]; National Natural Science Foundation of China [81971938]; Natural Science Foundation of Hainan Province [820QN269]; The Innovation Research Team for Basic and Clinical Studies on Chronic Liver Diseases of 2018 High-Level Health Teams of Zhuhai (for Y.-P.L.) [2018]

ORCID

Yi-Ping Li http://orcid.org/0000-0001-6011-3101

References

[1] WHO. WHO report on the Ten Threats to Global Health. https://www.who.int/news-room/spotlight/ten-threats-to-global-health-in-2019
[2] Wilder-Smith A, Ooi EE, Horstick O, et al. Dengue. Lancet. 2019 Jan 26;393(10169):350–363.
[3] Guzman MG, Halstead SB, Artsob H, et al. Dengue: a continuing global threat. Nat Rev Microbiol. 2010 Dec;8(12 Suppl):S7–16.
[4] Bhatt S, Gething PW, Brady OJ, et al. The global distribution and burden of dengue. Nature. 2013 Apr 25;496(7446):504–507.
[5] Guzman MG, Harris E. Dengue. Lancet. 2015 Jan 31;385(9966):453–465.
[6] Halstead SB. Dengue. Lancet. 2007 Nov 10;370(9599):1644–1652.
[7] Pierson TC, Diamond MS. The continued threat of emerging flaviviruses. Nat Microbiol. 2020 Jun;5(6):796–812.
[8] Kuhn RJ, Zhang W, Rossmann MG, et al. Structure of dengue virus: implications for flavivirus organization, maturation, and fusion. Cell. 2002 Mar 8;108(5):717–725.
[9] Iglesias NG, Gamarnik AV. Dynamic RNA structures in the dengue virus genome. RNA Biol. 2011 Mar-Apr;8(2):249–257.
[10] Diamond MS, Pierson TC. Molecular insight into dengue virus pathogenesis and its implications for disease control. Cell. 2015 Jul 30;162(3):488–492.
[11] Miller S, Krijnse-Locker J. Modification of intracellular membrane structures for virus replication. Nat Rev Microbiol. 2008 May;6(5):363–374.
[12] Welsch S, Miller S, Romero-Brey I, et al. Composition and three-dimensional architecture of the dengue virus replication and assembly sites. Cell Host Microbe. 2009 Apr 23;5(4):365–375.
[13] Chatel-Chaix L, Bartenschlager R. Dengue virus- and hepatitis C virus-induced replication and assembly compartments: the enemy inside–caught in the web. J Virol. 2014 Jun;88(11):5907–5911.
[14] Apte-Sengupta S, Sirohi D, Kuhn RJ. Coupling of replication and assembly in flaviviruses. Curr Opin Virol. 2014 Dec;9:134–142.
[15] Geddes K, Magalhaes JG, Girardin SE. Unleashing the therapeutic potential of NOD-like receptors. Nat Rev Drug Discov. 2009 Jun;8(6):465–579.
[16] Fritz JH, Ferrero RL, Philpott DJ, et al. Nod-Like proteins in immunity, inflammation and disease. Nat Immunol. 2006 Dec;7(12):1250–1257.
[17] Lupfer C, Kanneganti TD. The expanding role of NLRs in antiviral immunity. Immunol Rev. 2013 Sep;255(1):13–24.
[18] Yao Y, Qian Y. Expression regulation and function of NLRC5. Protein Cell. 2013 Mar;4(3):168–175.
[19] Kuenzel S, Till A, Winkler M, et al. The nucleotide-binding oligomerization domain-like receptor NLRC5 is involved in IFN-dependent antiviral immune responses. J Immunol. 2010 Feb 15;184(4):1990–2000.
[20] Chonwerawong M, Ferrand J, Chaudhry HM, et al. Innate immune molecule NLRC5 protects mice from helicobacter-induced formation of gastric lymphoid tissue. Gastroenterology. 2020 Jul;159(1):169–182 e8.
[21] Cui J, Zhu L, Xia X, et al. NLRC5 negatively regulates the NF-kappaB and type I interferon signaling pathways. Cell. 2010 Apr 30;141(3):483–496.
[22] Meng Q, Cai C, Sun T, et al. Reversible ubiquitination shapes NLRC5 function and modulates NF-κB activation switch. J Cell Biol. 2015 Dec 7;211(5):1025–1040.
[23] Tong Y, Cui J, Li Q, et al. Enhanced TLR-induced NF-κB signaling and type I interferon responses in NLRC5 deficient mice. Cell Res. 2012 May;22(5):822–835.
[24] Ranjan P, Singh N, Kumar A, et al. NLRC5 interacts with RIG-I to induce a robust antiviral response against influenza virus infection. Eur J Immunol. 2015 Mar;45(3):758–772.
[25] Wu XM, Hu YW, Xue NN, et al. Role of zebrafish NLRC5 in antiviral response and transcriptional regulation of MHC related genes. Dev Comp Immunol. 2017 Mar;68:58–68.
[26] Neerincx A, Lautz K, Menning M, et al. A role for the human nucleotide-binding domain, leucine-rich repeat-containing family member NLRC5 in antiviral responses. J Biol Chem. 2010 Aug 20;285(34):26223–26232.
[27] Yao Y, Wang Y, Chen F, et al. NLRC5 regulates MHC class I antigen presentation in host defense against intracellular pathogens. Cell Res. 2012 May;22(5):836–847.

[28] Meissner TB, Li A, Biswas A, et al. NLR family member NLRC5 is a transcriptional regulator of MHC class I genes. Proc Natl Acad Sci U S A. 2010 Aug 3;107(31):13794–13799.
[29] Yoo JS, Sasaki M, Cho SX, et al. SARS-CoV-2 inhibits induction of the MHC class I pathway by targeting the STAT1-IRF1-NLRC5 axis. Nat Commun. 2021 Nov 15;12(1):6602.
[30] Kumar H, Pandey S, Zou J, et al. NLRC5 deficiency does not influence cytokine induction by virus and bacteria infections. J Immunol. 2011 Jan 15;186(2):994–1000.
[31] Lamkanfi M, Kanneganti TD. Regulation of immune pathways by the NOD-like receptor NLRC5. Immunobiology. 2012 Jan;217 (1):13–16.
[32] Moy RH, Gold B, Molleston JM, et al. Antiviral autophagy restrictsRift Valley fever virus infection and is conserved from flies to mammals. Immunity. 2014 Jan 16;40(1):51–65.
[33] Dikic I, Elazar Z. Mechanism and medical implications of mammalian autophagy. Nat Rev Mol Cell Biol. 2018 Jun;19(6):349–364.
[34] Lin CY, Nozawa T, Minowa-Nozawa A, et al. Autophagy receptor tollip facilitates bacterial autophagy by recruiting galectin-7 in response to group a streptococcus infection. Front Cell Infect Microbiol. 2020 ;10:583137.
[35] Trelford CB, Di Guglielmo GM. Molecular mechanisms of mammalian autophagy. Biochem J. 2021 Sep 30;478(18):3395–3421.
[36] Behrends C, Sowa ME, Gygi SP, et al. Network organization of the human autophagy system. Nature. 2010 Jul 1;466(7302):68–76.
[37] Stolz A, Ernst A, Dikic I. Cargo recognition and trafficking in selective autophagy. Nat Cell Biol. 2014 Jun;16(6):495–501.
[38] He X, Zhu Y, Zhang Y, et al. RNF34 functions in immunity and selective mitophagy by targeting MAVS for autophagic degradation. Embo J. 2019 Jul 15;38(14):e100978.
[39] Jin S, Tian S, Luo M, et al. Tetherin suppresses type I interferon signaling by targeting MAVS for NDP52-mediated selective autophagic degradation in human cells. Mol Cell. 2017 Oct 19;68 (2):308–322 e4.
[40] Shaid S, Brandts CH, Serve H, et al. Ubiquitination and selective autophagy. Cell Death Differ. 2013 Jan;20(1):21–30.
[41] Talloczy Z, Virgin H, Levine B. PKR-Dependent autophagic degradation of herpes simplex virus type 1. Autophagy. 2006 Jan-Mar;2(1):24–29.
[42] Kim N, Kim MJ, Sung PS, et al. Interferon-Inducible protein SCOTIN interferes with HCV replication through the autolysosomal degradation of NS5A. Nat Commun. 2016 Feb 12;7:10631.
[43] Kong N, Shan T, Wang H, et al. BST2 suppresses porcine epidemic diarrhea virus replication by targeting and degrading virus nucleocapsid protein with selective autophagy. Autophagy. 2020 Oct;16(10):1737–1752.
[44] Sun MX, Huang L, Wang R, et al. Porcine reproductive and respiratory syndrome virus induces autophagy to promote virus replication. Autophagy. 2012 Oct;8(10):1434–1447.
[45] Liu Y, Cherry S. Zika virus infection activates sting-dependent antiviral autophagy in the Drosophila brain. Autophagy. 2019 Jan;15(1):174–175.
[46] He J, Yang L, Chang P, et al. Zika virus NS2A protein induces the degradation of KPNA2 (karyopherin subunit alpha 2) via chaperone-mediated autophagy. Autophagy. 2020 Dec;16 (12):2238–2251.
[47] Choi Y, Bowman JW, Jung JU. Autophagy during viral infection - a double-edged sword. Nat Rev Microbiol. 2018 Jun;16 (6):341–354.
[48] Zhao Y, Shao F. NLRC5: a NOD-like receptor protein with many faces in immune regulation. Cell Res. 2012 Jul;22 (7):1099–1101.
[49] Guo X, Liu T, Shi H, et al. Respiratory syncytial virus infection upregulates NLRC5 and major histocompatibility complex class I expression through RIG-I induction in airway epithelial cells. J Virol. 2015 Aug;89(15):7636–7645.
[50] Luo D, Xu T, Hunke C, et al. Crystal structure of the NS3 protease-helicase from dengue virus. J Virol. 2008 Jan;82(1):173–183.
[51] Pohl C, Dikic I. Cellular quality control by the ubiquitin-proteasome system and autophagy. Science. 2019 Nov 15;366(6467):818–822.
[52] Nedelsky NB, Todd PK, Taylor JP. Autophagy and the ubiquitin-proteasome system: collaborators in neuroprotection. Biochim Biophys Acta. 2008 Dec;1782(12):691–699.
[53] Li W, He P, Huang Y, et al. Selective autophagy of intracellular organelles: recent research advances. Theranostics. 2021;11 (1):222–256.
[54] Lu K, Psakhye I, Jentsch S. Autophagic clearance of polyQ proteins mediated by ubiquitin-Atg8 adaptors of the conserved CUET protein family. Cell. 2014 Jul 31;158(3):549–563.
[55] Xu Z, Yang L, Xu S, et al. The receptor proteins: pivotal roles in selective autophagy. Acta Biochim Biophys Sin (Shanghai). 2015 Aug;47(8):571–580.
[56] Deretic V, Saitoh T, Akira S. Autophagy in infection, inflammation and immunity. Nat Rev Immunol. 2013 Oct;13(10):722–737.
[57] Khaminets A, Behl C, Dikic I. Ubiquitin-Dependent and independent signals in selective autophagy. Trends Cell Biol. 2016 Jan;26 (1):6–16.
[58] Levine B, Mizushima N, Virgin HW. Autophagy in immunity and inflammation. Nature. 2011 Jan 20;469(7330):323–335.
[59] Travassos LH, Carneiro LA, Ramjeet M, et al. Nod1 and Nod2 direct autophagy by recruiting ATG16L1 to the plasma membrane at the site of bacterial entry. Nat Immunol. 2010 Jan;11(1):55–62.
[60] Lei Y, Wen H, Yu Y, et al. The mitochondrial proteins NLRX1 and TUFM form a complex that regulates type I interferon and autophagy. Immunity. 2012 Jun 29;36(6):933–946.
[61] Heaton NS, Randall G. Dengue virus-induced autophagy regulates lipid metabolism. Cell Host Microbe. 2010 Nov 18;8(5):422–432.
[62] Lennemann NJ, Coyne CB. Dengue and Zika viruses subvert reticulophagy by NS2B3-mediated cleavage of FAM134B. Autophagy. 2017 Feb;13(2):322–332.
[63] Lee YR, Kuo SH, Lin CY, et al. Dengue virus-induced ER stress is required for autophagy activation, viral replication, and pathogenesis both in vitro and in vivo. Sci Rep. 2018 Jan 11;8(1):489.
[64] Samsa MM, Mondotte JA, Iglesias NG, et al. Dengue virus capsid protein usurps lipid droplets for viral particle formation. PLoS Pathog. 2009 Oct;5(10):e1000632.
[65] Metz P, Chiramel A, Chatel-Chaix L, et al. Dengue virus inhibition of autophagic flux and dependency of viral replication on proteasomal degradation of the autophagy receptor p62. J Virol. 2015 Aug;89(15):8026–8041.
[66] Abernathy E, Mateo R, Majzoub K, et al. Differential and convergent utilization of autophagy components by positive-strand RNA viruses. PLoS Biol. 2019 Jan;17(1):e2006926.
[67] Li MY, Naik TS, Siu LYL, et al. Lyn kinase regulates egress of flaviviruses in autophagosome-derived organelles. Nat Commun. 2020 Oct 15;11(1):5189.
[68] Orvedahl A, Sumpter R Jr., Xiao G, et al. Image-Based genome-wide siRNA screen identifies selective autophagy factors. Nature. 2011 Dec 1;480(7375):113–117.
[69] Mandell MA, Jain A, Arko-Mensah J, et al. TRIM proteins regulate autophagy and can target autophagic substrates by direct recognition. Dev Cell. 2014 Aug 25;30(4):394–409.
[70] Du Pont KE, McCullagh M, Geiss BJ. Conserved motifs in the flavivirus NS3 RNA helicase enzyme. Wiley Interdiscip Rev RNA. 2021 Sep 2;13:e1688. DOI:10.1002/wrna.1688.
[71] Lescar J, Luo D, Xu T, et al. Towards the design of antiviral inhibitors against flaviviruses: the case for the multifunctional NS3 protein from dengue virus as a target. Antiviral Res. 2008 Nov;80(2):94–101.
[72] Gandikota C, Mohammed F, Gandhi L, et al. Mitochondrial import of dengue virus NS3 protease and cleavage of GrpEL1, a cochaperone of mitochondrial Hsp70. J Virol. 2020 Aug 17;94 (17):e01178–20.

[73] Chiramel AI, Meyerson NR, McNally KL, et al. Trim5alpha restricts flavivirus replication by targeting the viral protease for proteasomal degradation. Cell Rep. 2019 Jun 11;27(11):3269–3283 e6.
[74] Clum S, Ebner KE, Padmanabhan R. Cotranslational membrane insertion of the serine proteinase precursor NS2B-NS3(Pro) of dengue virus type 2 is required for efficient in vitro processing and is mediated through the hydrophobic regions of NS2B. J Biol Chem. 1997 Dec 5;272(49):30715–30723.
[75] Brady OJ, Gething PW, Bhatt S, et al. Refining the global spatial limits of dengue virus transmission by evidence-based consensus. PLoS Negl Trop Dis. 2012;6(8):e1760.
[76] Aguirre S, Luthra P, Sanchez-Aparicio MT, et al. Dengue virus NS2B protein targets cGAS for degradation and prevents mitochondrial DNA sensing during infection. Nat Microbiol. 2017 Mar 27;2:17037.
[77] Gebhard LG, Iglesias NG, Byk LA, et al. A proline-rich N-terminal region of the dengue virus NS3 is crucial for infectious particle production. J Virol. 2016 Jun 1;90(11):5451–5461.
[78] Wang K, Zou C, Wang X, et al. Interferon-Stimulated TRIM69 interrupts dengue virus replication by ubiquitinating viral nonstructural protein 3. PLoS Pathog. 2018 Aug;14(8):e1007287.
[79] Bagga T, Tulsian NK, Mok YK, et al. Mapping of molecular interactions between human E3 ligase TRIM69 and dengue virus NS3 protease using hydrogen-deuterium exchange mass spectrometry. Cell Mol Life Sci. 2022 Apr 10;79(5):233.
[80] Panayiotou C, Lindqvist R, Kurhade C, et al. Viperin restricts zika virus and tick-borne encephalitis virus replication by targeting NS3 for proteasomal degradation. J Virol. 2018 Apr 1;92(7):e02054–17.
[81] Wu Y, Yang X, Yao Z, et al. C19orf66 interrupts Zika virus replication by inducing lysosomal degradation of viral NS3. PLoS Negl Trop Dis. 2020 Mar;14(3):e0008083.
[82] Zellner S, Schifferer M, Behrends C. Systematically defining selective autophagy receptor-specific cargo using autophagosome content profiling. Mol Cell. 2021 Mar 18;81(6):1337–1354 e8.
[83] Herhaus L, Dikic I. Expanding the ubiquitin code through post-translational modification. EMBO Rep. 2015 Sep;16(9):1071–1083.
[84] Song L, Luo ZQ. Post-Translational regulation of ubiquitin signaling. J Cell Biol. 2019 Jun 3;218(6):1776–1786.
[85] Chen M, Meng Q, Qin Y, et al. TRIM14 inhibits cGAS degradation mediated by selective autophagy receptor p62 to promote innate immune responses. Mol Cell. 2016 Oct 6;64(1):105–119.
[86] Chen YH, Huang TY, Lin YT, et al. VPS34 K29/K48 branched ubiquitination governed by UBE3C and TRABID regulates autophagy, proteostasis and liver metabolism. Nat Commun. 2021 Feb 26;12(1):1322.
[87] Kim HJ, Kim SY, Kim DH, et al. Crosstalk between HSPA5 arginylation and sequential ubiquitination leads to AKT degradation through autophagy flux. Autophagy. 2021 Apr;17(4):961–979.
[88] Pu SY, Wu RH, Tsai MH, et al. A novel approach to propagate flavivirus infectious cDNA clones in bacteria by introducing tandem repeat sequences upstream of virus genome. J Gen Virol. 2014 Jul;95(Pt 7):1493–1503.
[89] Zheng Y, Liu Q, Wu Y, et al. Zika virus elicits inflammation to evade antiviral response by cleaving cGAS via NS1-caspase-1 axis. Embo J. 2018 Sep 14;37(18):e99347.
[90] Wu Y, Jin S, Liu Q, et al. Selective autophagy controls the stability of transcription factor IRF3 to balance type I interferon production and immune suppression. Autophagy. 2021 Jun;17(6):1379–1392.